C1

Activation of the epithelial sodium channel (ENaC) by extracellular proteases critically involves a putative prostasin cleavage site in the channel's γ-subunit

A. Diakov, K. Aspden, M. Mokrushina, B. Krüger and C. Korbmacher

Institute of Cellular and Molecular Physiology, University of Erlangen-Nurmberg, Erlangen, Germany

The epithelial sodium channel (ENaC) is the rate limiting step for sodium absorption in the aldosterone sensitive distal nephron. The appropriate regulation of renal ENaC activity is critically important for the maintenance of body sodium balance and hence for the long term regulation of arterial blood pressure. Proteolytic cleavage by intra- and extracellular proteases is thought to contribute to ENaC processing and regulation under physiological and pathophysiological conditions (Rossier 2004). Proteases acting from the extracellular side have been shown to activate near-silent channels in the plasma membrane (Caldwell *et al.* 2004). However, the underlying molecular mechanisms are not yet fully understood. We used trypsin, chymotrypsin and human neutrophil elastase (hNE) as tools to activate rat ENaC heterologously expressed in *Xenopus laevis* oocytes. Trypsin application increased ENaC whole-cell currents about 8-fold without a concomitant increase in channel surface expression. The stimulatory effect of trypsin was preserved in oocytes expressing αγENaC, but was abolished in oocytes expressing αβENaC. Thus, the γ subunit appears to be essential for channel activation by exogenous proteases. In single channel recordings from outside-out patches from oocytes expressing αβγENaC we demonstrated that trypsin (*i*) increases the open probability (P_O) of channels that are already active and (*ii*) activates a population of near-silent channels. This dual effect was confirmed by experiments using the β518C mutant ENaC which can be converted to a channel with a P_O of nearly one by exposure to a sulfhydryl reagent. Site-directed mutagenesis of a recently identified putative prostasin cleavage site in the extracellular loop of the γ subunit (Bruns *et al.* 2007) revealed that mutating the 181Lys residue to alanine (γK181A) largely reduces the stimulatory effect of extracellular proteases (trypsin, chymotrypsin and hNE), increases ENaC baseline whole-cell currents, and decreases channel surface expression. Moreover, the γK181A mutation promotes the spontaneous appearance of a 67 kDa fragment of the γ-subunit which also appears after channel activation by extracellular trypsin. At the single-channel level the γK181A mutation essentially abolishes the activation of near-silent channels by trypsin, while the stimulatory effect of trypsin on the P_O of active channels is preserved. We conclude that the putative prostasin cleavage site in the γ-subunit of ENaC is functionally important for the activation of near-silent channels by extracellular proteases.

Bruns JB, Carattino MD, Sheng S, Maarouf AB, Weisz OA, Pilewski JM, Hughey RP & Kleyman TR (2007). *J Biol Chem* **282**, 6153-6160.

Caldwell RA, Boucher RC & Stutts MJ (2004). *Am J Physiol Cell Physiol* **286**, C190-194.

Rossier BC (2004). *Proc Am Thorac Soc* **1**, 4-9.

Supported by the Deutsche Forschungsgemeinschaft (SFB 423 TPA12; C.K.) and by the DAAD (M.M).

Where applicable, the authors confirm that the experiments described here conform with The Physiological Society ethical requirements.

C2

Transfer of H^+-gating properties by exchanging pH sensors between two-pore domain K^+ channels of the TASK and TALK subfamilies

L. Zúñiga[1,2], F.D. González-Nilo[3], W. González[3], L. Cid[1], F.V. Sepúlveda[1] and M. Niemeyer[1]

[1]Centro de Estudios Científicos (CECS), Valdivia, Chile, [2]Universidad Austral, Valdivia, Chile and [3]Centro de Bioinformática y Simulación Molecular, Universidad de Talca, Talca, Chile

Potassium channels share a common selectivity filter and their diversity is given by how they are gated open. TASK-2 (K2P5.1) and TASK-3 (K2P9.1) are two-pore-domain K^+ channels gated by extracellular pH (pH_o), which play important roles in renal bicarbonate reabsorption (Warth et al. 2004) and excitability (Brickley et al. 2007) respectively. Whilst TASK-3, a TASK subfamily member, is inhibited by lowering pH_o, the TALK subfamily member TASK-2 is activated by alkalinization. The molecular determinants of pH_o-gating for these channels have been identified. TASK-3 senses pH_o through pore-mouth residue H98 (N103 in TASK-2) (Kim et al. 2000; Rajan et al. 2000). Sensing of pH_o in TASK-2 is believed to take place at R224 (V221 in TASK-3) located in the outermost portion of helix TM4 near the channel pore (Niemeyer et al. 2007). The unusual pK_a of 8.0 of the arginine sensor in TASK-2 has been attributed to its hydrophobic environment. Mutation of sensor residues of TASK-2 and -3 to neutral amino acids abolishes pH_o sensitivity. Here we report patch-clamp experiments using the recombinant channels to analyse the result of pH_o-sensor transplantation between TASK-2 and TASK-3 further to validate their identification. The position equivalent to TASK-2 R224 is occupied by V221 in TASK-3. Replacing this residue by a titratable histidine (to facilitate protonation-deprotonation at near-physiological pH) in the background of the pH_o-insensitive TASK-3-H98N led to a recovery of pH_o-sensitivity. The observed pK_a values were 6.0±0.1 (mean ± SEM, n= 8) for the WT TASK-3 and 6.9±0.1 (n=7) for the double mutant TASK-3-H98N-V221H. The Hill coefficient n_H was decreased from a value of 2.1±0.1 to 0.65±0.1, near that for TASK-2, in the double mutant. The K^+/Na^+ selectivity was also decreased in TASK-3-H98N-V221H, suggestive of an electrostatic effect leading to some form of pore collapse induced by the presence of the positively charged residue at position 221 in TASK-3. The position equivalent to TASK-3 H98 is occupied by N103 in TASK-2. The mutation of N103 for H, to create a TASK-3 sensor in the background of pH_o-insensitive TASK-2-R224A also restored H^+-gating in this mutant. The observed pK_a values were 8.0 ± 0.1 (n= 6) for WT TASK-2 and 7.6 ± 0.1 (n=7) for the double mutant TASK-2-R224A-N103H. Our results support the idea that R224 acting with a markedly shifted pK_a is the pH_o sensor of TASK-2. The protonation-deprotonation of R224 would have a direct effect on the electrostatic potential of

the selectivity filter and would regulate open probability at the pore by modulating K^+ occupancy.

Brickley SG, Aller MI, Sandu C, Veale EL, Alder FG, Sambi H, Mathie A, & Wisden W (2007). J Neurosci 27, 9329-9340.

Kim Y, Bang H, & Kim D (2000). J Biol Chem 275, 9340-9347.

Niemeyer MI, González-Nilo FD, Zúñiga L, González W, Cid LP, & Sepúlveda FV (2007). Proc Natl Acad Sci U S A 104, 666-671.

Rajan S, Wischmeyer E, Liu GX, Preisig-Muller R, Daut J, Karschin A, & Derst C (2000). J Biol Chem 275, 16650-16657.

Warth R, Barrière H, Meneton P, Bloch M, Thomas J, Tauc M, Heitzmann D, Romeo E, Verrey F, Mengual R, Guy N, Bendahhou S, Lesage F, Poujeol P, & Barhanin J (2004). Proc Natl Acad Sci U S A 101, 8215-8220.

Where applicable, the authors confirm that the experiments described here conform with The Physiological Society ethical requirements.

C3

Sodium-dependent regulation of ENaC by apical P2 receptors in rat collecting duct: are P2X receptors luminal sodium sensors?

S.S. Wildman[1,2], D.G. Shirley[2], B.F. King[2] and R.J. Unwin[2]

[1]Veterinary Basic Sciences, Royal Veterinary College, London, UK and [2]Physiology and Nephrology, UCL, London, UK

The epithelial Na^+ channel (ENaC) plays a major role in the regulation of Na^+ balance and blood pressure by controlling Na^+ reabsorption along the renal collecting duct (CD). ENaC activity is inhibited by P2 receptors (P2Rs) which are activated by extracellular nucleotides. However, uncertainties exist over the mechanism of inhibition, the P2R subtype(s) involved and molecular pathway(s) activated. This study has addressed the relationship between apical P2Rs and ENaC inhibition in the rat CD.

Kidneys from terminally anaesthetized adult Sprague-Dawley rats, which had been maintained on a low (0.01%) Na^+ diet (for 10-days in order to increase CD ENaC expression), were microdissected and isolated CD segments were split-open to expose the apical membrane of individual principal cells (PCs). PCs (*in situ*) were studied under voltage-clamp conditions (V_h = -60 mV) using the whole-cell perforated-patch clamp technique.

Apically-applied ATP, ATPγS, UTP and 2meSATP each evoked inward currents (≤500 pA; 10 μM; n = 10), whereas 2meSADP and BzATP were inactive (10 μM; n = 10). Currents evoked by 2meSATP were insensitive to DIDS (100 μM; n = 5) and shown to be cationic, consistent with P2X channel activation. Currents evoked by UTP were abolished by DIDS (n = 5), consistent with P2Y receptor activation of Ca^{2+}-dependent Cl^- currents.

Within 3 minutes, nucleotide evoked inward currents significantly reduced the amplitude of subsequent ENaC-mediated currents over a wide range of holding voltages (between 30-60%; $P<0.05$) without changing the inward rectification or reversal potential (n = 12). Lowering extracellular Na^+ concentration from 145 to 50 mM failed to alter the degree of inhibition caused by UTP-evoked currents, however 2meSATP-evoked responses instead potentiated the amplitude of the ENaC-mediated current-voltage relationships (75%; n = 7). 2meSATP-mediated potentiation of ENaC currents was abolished by wortmannin (100 nM; n = 3).

When taken together with previously reported immunohistochemical data (Chapman *et al.* 2006), these biophysical and pharmacological data suggest that ENaC activity is inhibited by apical $P2Y_{2\ and/or\ 4}$ and $P2X_{4\ and/or\ 4/6}$ receptors when extracellular Na^+ concentrations are high (145 mM; n = 12) but apical $P2X_{4\ and/or\ 4/6}$ receptors switch to potentiators of ENaC activity (involving PI3K) when extracellular Na^+ is lowered (to 50 mM; n = 5). We propose that $P2X_{4\ and/or\ 4/6}$ receptors function as apical Na^+ sensors responsible for local regulation of ENaC activity in the CD and could thereby regulate Na^+ balance and systemic blood pressure.

Chapman *et al.* (2006) *Proc Physiol Soc* 2, PC7.

Supported by British Heart Foundation and St Peter's Trust.

Where applicable, the authors confirm that the experiments described here conform with The Physiological Society ethical requirements.

C4

Imaging primary cilia on MDCK cells using atomic force microscopy

J. Evangelides[1], D.N. Sheppard[2] and T.J. McMaster[1]

[1]H. H. Wills Physics Laboratory, University of Bristol, Bristol, UK and [2]Department of Physiology and Pharmacology, University of Bristol, Bristol, UK

Primary cilia are solitary, immotile, hair-like structures that protrude from the apical membrane of kidney epithelial cells into the cavity of the nephron. The function of the primary cilia was originally unknown, however recent work [1] has identified a link between primary cilia malfunction and autosomal dominant polycystic kidney disease (ADPKD). This malfunction suggests these organelles might act as flow sensors, signalling changes in luminal flow to control transepithelial ion transport along the nephron. Here we have adopted an interdisciplinary approach to investigate the structure and functionality of the primary cilium. We have imaged both Type I and Type II MDCK cells, using scanning electron microscopy (SEM) and atomic force microscopy (AFM). Cells were grown on glass coverslips and fixed with 2% glutaraldehyde in PBS. SEM was used to observe the density of cells and cilia, prior to AFM images being obtained of primary cilia on Type II MDCK cells.

Live cells were imaged under liquid, and as the cilia remain mobile and not adherent to a substrate, their movement and orientation may affect the motion of the AFM cantilever. We found that it was possible to image unfixed cilia using AFM, by removing the cilia from the cell surface. We have achieved this by using

a 'peel-off' method [2] whereby a poly-L-lysine-coated coverslip, placed on top of a layer of cells in a Petri dish, is removed in a single movement, and then imaged *in situ*. The nanoscale surface structure of the immobilised cilia can then be imaged with the AFM. From an analysis of AFM data, we have estimated cilium flexibility, and have probed cilium elasticity using AFM in a nanomechanical mode. By correlating AFM images with single-point AFM force curves, we observe a clear difference in stiffness between the cilium and the cell surface.

Using a combined AFM/confocal microscope we have correlated the structures imaged by AFM, to fluorescent markers for tubulin and actin. The staining observed by confocal microscopy confirms that the structures protruding from the cells in the AFM images are the primary cilia. In a further development, we will report preliminary results from a combination of AFM imaging and patch-clamp electrophysiology to probe how cilium bending is coupled to ion transport.

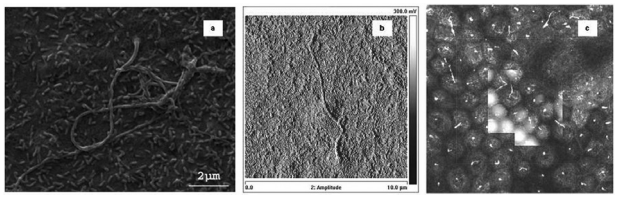

(a) SEM image (2 µm) of primary cilia on fixed MDCK cells; (b) AFM image (10 µm) of primary cilia on fixed MDCK cells; and (c) Combined confocal (immunofluorescence for tubulin and actin) and AFM images, the latter present as an overlay in the centre of the confocal image.

1. Ong AC and DN Wheatley (2003). The Lancet 361(9359), 774-776.

2. Huang BQ et al. (2006). Am J Physiol Gastrointest Liver Physiol 291, G500-509.

Where applicable, the authors confirm that the experiments described here conform with The Physiological Society ethical requirements.

C5

The cilium-dependent flow-response is amplified by nucleotide release in MDCK cells

H. Praetorius and J. Leipziger

Institute for Physiology and Biophysics, University of Aarhus, Aarhus, Denmark

Cultured renal epithelial cells sense changes in fluid flow by their primary cilia (1). Freshly isolated renal tubules also respond changes in fluid flow by transient increases in the intracellular Ca^{2+} concentration, $[Ca^{2+}]_i$. The signal transduction pathway is, however, not well defined. Mechanical stimulation in general is known to promote release of nucleotides (ATP/UTP) and triggers auto- and paracrine activation of P2 receptors in renal epithelia. Recently, we showed that the flow-induced $[Ca^{2+}]_i$ response in freshly isolated medullary thick ascending limb (mTAL) involves mechanically stimulated nucleotide release (2). The flow/pressure induced response was abolished by scavenging of ATP (apyrase) and by the un-selective P2-receptor antagonist (suramin). In addition, the flow/pressure induced response was strikingly lower in mice lacking the P2Y2 receptor, the predominant P2 receptor in mTAL. Our results strongly suggest that the flow-induced response is caused by release of bilateral nucleotides and subsequent activation of P2 receptors.

It is, however, not known if the primary cilium is necessary for this type of response. Here, we study the influence of extracellular nucleotides on the cilium dependent flow-response and address whether ATP is released during the course of the response. We used MDCK cells in a semi-open perfusion chamber model, where the flow response is known to be absolutely cilium-dependent at low flow rates. (A) We show that the epithelial sensitivity to changing flow rates is increased at low concentrations of nucleotides that do not by themselves induce $[Ca^{2+}]_i$ elevations. (B) Scavenging of ATP with apyrase (10U/ml) reduced the cilium-dependent flow response by 56.2%, whereas desensitisation of apical P2 receptors with ATP did not affect the response. (C) Non-ciliated MDCK cells, which do not respond to changes in fluid flow were used as reporter cells for paracrine ATP signalling. MDCK cells were grown on half coverslips and the non-confluent indicator cells were positioned on the outflow side, directly next to the confluent cells. Intriguingly, the non-ciliated cells only responded to fluid flow with confluent ciliated cells on the inflow side (fig.). This was not the case if non-confluent, non-ciliated cells were placed on the inflow side. This paracrine response was reduced by scavenging of ATP. The data allow us to conclude that flow-induced, primary cilia-dependent $[Ca^{2+}]_i$ signalling is potentiated by stimulated nucleotide release.

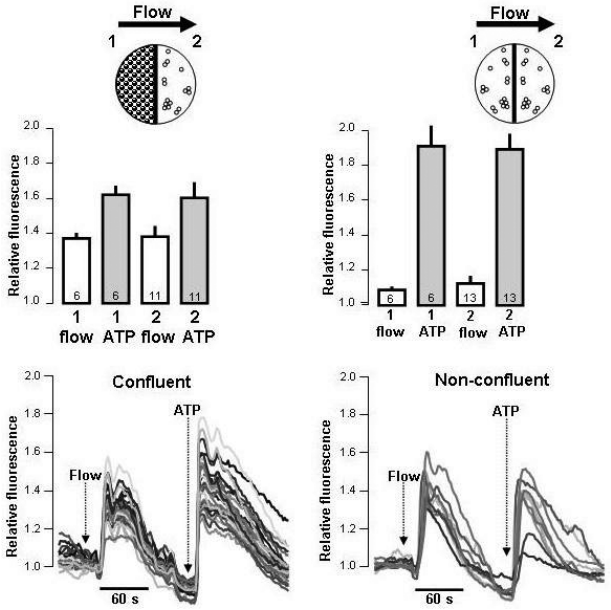

Praetorius HA & Spring KR (2001). J Membr Biol 184, 71-79.

Jensen ME, Odgaard E, Christensen MH, Praetorius HA & Leipziger J (2007). J Am Soc Nephrol 18, 2062-2070.

Where applicable, the authors confirm that the experiments described here conform with The Physiological Society ethical requirements.

C6

Phosphorylation of Kidney Anion Exchanger 1 (Band 3) on tyrosine residues Y359 and Y904 critical for basolateral trafficking

A.M. Toye, A.C. Brown, W.J. Mawby and R.C. Williamson

Biochemistry, University of Bristol, Bristol, UK

The human Anion exchanger 1 (AE1, band 3, SLC4A1) is highly expressed in erythrocytes and ∝-intercalated cells of the kidney. The kidney AE1 (kAE1) is a truncated version of AE1 found in the basolateral membrane and its correct localisation and function is essential for renal acid secretion. However, despite its importance in whole body pH homeostasis surprisingly little is known about the trafficking and regulation of human kAE1.

We have developed a polarisable cell model system expressing human kAE1 in MDCKI cells (MDCKI-kAE1 cells) to investigate the regulation of the trafficking of kAE1. We have already shown, using this model system, that the C-terminal tyrosine residue (Y904) is critical for basolateral localisation in polarised cells and that the N-terminus of kAE1 is also essential for polarized trafficking. We have now utilized mutagenesis to further investigate the regions of the N-terminus important for kAE1 trafficking. In particular, we have found that the Y359A mutant is mistargeted to the apical membrane. Therefore, kAE1 has a requirement for the presence of both Y359 in the N-terminus and Y904 in the C-terminus for correct trafficking.

Tyrosine phosphorylation can influence the localisation of proteins by regulating interactions with cellular targeting and/or internalisation machinery. Both Y359 and Y904 are phosphorylated in erythrocyte AE1. We show by cellular imaging and western blotting techniques using novel phosphotyrosine-specific antibodies raised against AE1 phosY359 and AE1 phosY904, that both Y359 and Y904 are phosphorylated in pervanadate treated MDCK-kAE1 cells. This phosphorylation was sensitive to Src kinase inhibitors. Therefore since both Y359 and Y904 are critical for basolateral targeting, we propose that reversible phosphorylation provides a means of regulating kAE1 trafficking to the basolateral membrane. We suggest that intercalated cells can regulate the levels and subcellular distribution of kAE1 in response to cellular stimuli and cues (such as acidosis or alkalosis) by reversible phosphorylation of Y359 and Y359. We are now exploring a range of stimuli to determine the physiological signals that influence kAE1 phosphorylation and their effects on basolateral localisation.

Funded by a NHS Blood and Transplant Wellcome Trust Career Development Fellowship and a Kidney Research UK and GSK PhD Studentship.

Where applicable, the authors confirm that the experiments described here conform with The Physiological Society ethical requirements.

C7

Evidence against ClC-5 as an electrical shunt in endosomal acidification in the proximal tubule

J.D. Lippiat and A.J. Smith

Institute of Membrane & Systems Biology, University of Leeds, Leeds, UK

ClC-5 is a member of the mammalian family of voltage-dependent Cl^- channels that acts as a Cl^-/H^+ exchanger (Picollo & Pusch, 2005; Scheel et al. 2005). Inherited mutations of *CLCN5* lead to defective albumin reabsorption in the proximal tubule (Dent's disease). At the cellular level, ClC-5 co-localises with v-ATPase in endosomes of the proximal tubule epithelial cells, where it is thought to provide a Cl^- conductance to counterbalance the active transport of H^+ into the endosomal lumen (Günther et al. 1998). Whether the physiological properties of ClC-5 permit this shunting role has yet to be fully addressed.

We transfected human embryonic kidney cells (HEK 293) with plasmid DNA encoding EYFP-tagged ClC-5 and recorded currents using the whole-cell patch clamp technique. The bath solution contained (in mM) 140 CsCl, 1 $CaCl_2$, 1 $MgCl_2$, and 10 HEPES, and the pipette solution contained 42 CsCl, 98 aspartate, 10 EGTA, and 10 HEPES; both solutions adjusted to pH 7.4. Cells were held at -30mV and 10ms pulses were applied from -100 to +200mV. Cells expressing ClC-5-EYFP produced outwardly-rectifying currents with a half-maximal activation voltage of +110 ± 2mV and an equivalent gating charge of 1.32 ± 0.13 (mean ± s.e.m., n=5). These currents, when extrapolated to the endosomal membrane, correspond to a unidirectional flux of chloride from the lumen to the cytosol. Currents were measured with $[Cl^-]$ ranging from 10 to 140mM and pH from 8.4 to 5.4 on both sides of the membrane, but on no occasion were inward currents observed.

To further understand the physiological role of ClC-5 in endosomal membranes we studied acidification using a pH-sensitive fluorescent protein, pHluorin, targeted to endosomes by fusion to VAMP2 (Miesenbock et al., 1998). In an extracellular buffer with pH 7.4, untransfected HEK cells acidified endosomal contents to pH 6.98 ± 0.05 (n=25), but failed to acidify endosomes (pH 7.40 ± 0.08, n=15) in the presence of 25μM bafilomycin, a v-ATPase inhibitor. HEK cells expressing ClC-5 had endosomal pH 6.41 ± 0.18 (n=30) and in the presence of bafilomycin, pH 6.87 ± 0.18 (n=16), indicating a bafilomycin-insensitive acidification mechanism when ClC-5 is present.

The data suggest that, in endosomes, ClC-5 does not act as en electrical shunt, but conducts Cl^- ions from the lumen to the cytosol. Since this is coupled to an exchange for H+ this may provide an acidification mechanism that acts in parallel with vesicular v-ATPase. This enhanced acidification in early endocytic vesicles may be important for efficient albumin endocytosis in the proximal tubule.

Picollo A & Pusch M (2005). Nature 436, 420-423.

Scheel O, et al. (2005). Nature 436, 424-427.

Günther et al. (1998). PNAS 95, 8075-8080.

Miesenbock G et al. (1998). Nature 394, 192-195.

Supported by The Wellcome Trust. We thank Prof. R.V. Thakker for the ClC-5 clone.

Where applicable, the authors confirm that the experiments described here conform with The Physiological Society ethical requirements.

C8

A range of functional consequences caused by Dent's disease missense mutations of ClC-5

A.J. Smith[1], A.A. Reed[2], N.Y. Loh[2], R.V. Thakker[2] and J.D. Lippiat[1]

[1]Institute of Membrane and Systems Biology, University of Leeds, Leeds, UK and [2]Academic Endocrine Unit, University of Oxford, Oxford, UK

ClC-5 is a member of the voltage-gated chloride channel family that acts as a Cl^-/H^+ antiporter [1,2]. It is expressed in the proximal tubule of the kidney where it involved in small-peptide reabsorption from the urine. ClC-5 is predominantly located on endosomal membranes and has been proposed to provide a Cl^- conductance to counterbalance the action of v-ATPase. Mutation of ClC-5 has been linked to Dent's disease, an X-linked disorder characterised by proteinurea, hypercalciurea and nephrolithiasis [3].

We have examined the functional consequences of several known Dent's disease missense mutations. Data are expressed as mean ± s.e.m., statistical significance determined by ANOVA. Following expression of wild-type (WT) and mutant EYFP-tagged ClC-5 in HEK293 cells, whole-cell currents were examined by patch-clamp electrophysiology. Current densities of cells expressing the G57V mutant (269±30pA/pF) were not different to WT (319±45pA/pF) ($p>0.05$, n=5) whereas R280P exhibited currents that were reduced by ~50% (155±46pA/pF) ($p<0.05$; n=5). Whole-cell currents of 5 other mutants (S270R, G513E, R516W, I524K & E527D) were not different to untransfected cells ($p<0.05$; n≥5). Confocal imaging of cells showed that WT, G57V, R280P and E527D were located predominantly in intracellular endosomes and to varying extents at the cell surface. The four remaining mutants were retained in the endoplasmic reticulum. Endocytosis was examined in cells expressing WT and endosome-targeted mutant ClC-5. The uptake of fluorescently-conjugated albumin was increased ~5-fold in cells expressing WT, G57V or R280P versus untransfected ($p<0.01$; n≥6) but not in E527D expressing cells ($p>0.05$; n=11). Uptake of fluorescently-conjugated dextran and transferrin were not affected by the presence of ClC-5 ($p>0.05$ vs untransfected; n≥4). Endosomal acidification was assayed using ratiometric pHluorin fused to VAMP2 for endosomal targeting [4]. Endosomes of untransfected cells bathed in pH 7.4 buffer were acidified to pH 6.98 ± 0.05. Significant acidification was observed in cells expressing WT (pH 6.40 ± 0.17), G57V (pH 6.25 ± 0.19) and R280P (pH 5.46 ± 0.15) ($p<0.01$ vs untransfected; n≥15 cells for each). Acidification in cells expressing E527D was impaired leading to a modest alkalisation compared to untransfected cells (pH 7.55 ± 0.09) ($p<0.05$; n=15 cells).

These data suggest that Dent's disease does not necessarily result from a loss of a ClC-5 conductance from the endosome, but could be caused by disruption of another unidentified process involving ClC-5. They also suggest that efficient albumin endocytosis requires functional ClC-5 at both surface and endosomal membranes.

Picollo A & Pusch M (2005). *Nature.* **436**. 420-423

Scheel O, *et al.* (2005). *Nature.* **436**. 424-427

Lloyd SE, *et al.* (1996). *Nature.* **379**. 445-449

Miesenbock G, *et al.* (1998). *Nature.* **394**. 192-195

Supported by the Wellcome Trust

Where applicable, the authors confirm that the experiments described here conform with The Physiological Society ethical requirements.

C9

Role of WT1 in the regulation of expression of pro- and anti-angiogenic isoforms of VEGF

E. Amin[1,2], D.G. Nowak[2,1], S.J. Harper[2], D.O. Bates[2] and M.R. Ladomery[1]

[1]Centre for Research in Biomedicine, University of the West of England, Bristol, UK and [2]Microvascular Research Laboratories, University of Bristol, Bristol, UK

The Wilms tumour suppressor gene WT1 is mutated in 10-15% of Wilms tumours and mutations in WT1 are also associated with Denys Drash Syndrome (DDS). DDS is characterised by childhood nephrotic syndrome, glomerulosclerosis, end-stage renal failure and Wilms tumours. WT1 encodes a zinc finger transcription factor that also regulates gene expression at the mRNA level. The search for WT1's DNA and mRNA targets is ongoing – a recent report has suggested that WT1 regulates the expression of a key growth factor, VEGF (Vascular Endothelial Growth Factor). There are two families of VEGF isoforms; an angiogenic family ($VEGF_{xxx}$); and a sister family of anti-angiogenic isoforms ($VEGF_{xxx}b$) that result from a distal alternative 3' splice site in exon 8 (Bates et al 2002). Although WT1 regulates VEGF expression transcriptionally, the extent to which WT1 affects VEGF isoform levels is not known, but splicing is altered in Denys Drash patients (Schumacher et al 2007). We measured VEGF isoform expression in differentiated wild-type and DDS patient-derived podocytes with a mutation in WT1 (R366C). The differentiated podocytes represents the closest in vivo model of podocytes in the kidney within the constraints of a cell culture model. Total VEGF and $VEGF_{xxx}b$ levels were determined by ELISA and RT-PCR. In the differentiated DDS podocytes there was a 0.13 ±0.002 fold reduction in the amount of $VEGF_{xxx}b$ compared to wildtype differentiated podocytes while DDS stably transfected with wildtype WT1 restored the expression of $VEGF_{xxx}b$ to 0.73 ±0.08. In the differentiated DDS podocytes there was a 2.32 ±0.483 fold increase in the amount of panVEGF compared to wildtype differentiated podocytes. Transfection of the wildtype WT1 into the differentiated DDS podocytes manages to rescue the DDS phenotype by decreasing the amount of panVEGF to 0.618 ±0.114 fold compare to wildtype podocytes. These results suggest that WT1 plays a role in the regulation of VEGF isoform expression; either by direct binding to VEGF pre-mRNA or by modulating splice factor activities

pletely reversible on washout of Al^{3+} with V_{hold} at 0mV but subsequent activation of CaCC was ~four fold faster. Finally, 1mM Al^{3+} failed to inhibit the pre-activated Cl^- conductance at 0mV. Taken together these data indicate that Al^{3+} blocks the depolarisation-induced activation of CaCC, but Al^{3+} has no direct blocking effect on the activated Cl^- conductance itself. This suggests that the physiological role of tpc1 is to act as the voltage-sensor upon membrane depolarisation to regulate CaCC in the apical membrane of IMCD cells.

Kawano T, Kadano T, Fumoto K, Lapeyrie F, Kuse M, Osobe M, Furuichi T, Muto S (2004). Biochem Biophys Res Comm 324, 40-45.

Sayer JA, Carr G, Morgan EL, Kellett GL, Simmons NL (2006). Proc Physiol Soc 2, PC22.

Stewart GS, Glanville M, Aziz O, Simmons NL Gray MA (2001). J Membrane Biol 180, 49-64.

Supported by Kidney Research UK.

Where applicable, the authors confirm that the experiments described here conform with The Physiological Society ethical requirements.

PC8

A comparison of P2 receptor mRNA expression levels in the renal collecting duct in response to altered dietary sodium and in DOCA-induced hypertension

L. Yew-Booth[2], M. Le Bras[2], S. Balesaria[2], J. Marks[2], C.M. Turner[2], D.G. Shirley[2], R.J. Unwin[2] and S.S. Wildman[1,2]

[1]Veterinary Basic Sciences, Royal Veterinary College, London, UK and [2]Physiology, Nephrology and Biochemistry, UCL, London, UK

The epithelial Na^+ channel (ENaC) is a regulated pathway for Na^+ uptake across the luminal membrane of the renal collecting duct (CD) and plays an important role in blood pressure control. Activation of many P2 receptor (P2R) subtypes (including: $P2X_{2,4,2/6 \text{ and/or } 4/6}$ and $P2Y_{2 \text{ and/or } 4}$) expressed in CD epithelial cells can alter ENaC activity in different ways (Wildman *et al.* 2005, 2007). It is known that changes in ENaC activity - when co-expressed in *Xenopus* oocytes or following dietary Na^+ restriction in native CD tissue - affects the expression levels of some P2Rs ($P2X_{1,2,4,5 \text{ and } 6}$ subunits and $P2Y_4$) (Wildman *et al.* 2005; 2007). We have proposed that P2Rs may locally regulate ENaC activity in the CD and that some P2Rs could be involved in the pathogenesis of hypertension. To examine the relationship between P2Rs and ENaC in the CD we have investigated P2R mRNA levels in CDs from adult Sprague-Dawley rats maintained on 'low' (0.01%), 'normal' (0.5%) or 'high' (4%) Na^+ diets (10 days) to alter ENaC expression and activity, and in DOCA-salt hypertensive rats (unilateral nephrectomy and DOCA treatment for 5 weeks; SBP = 189±12 $mmHg^{-1}$, n = 6). Kidneys from terminally anaesthetized rats were microdissected and CDs isolated (~15 mm; n = 6 for each sample). RNA was extracted and reverse transcribed, and the cDNA transcripts used for real time-PCR. A ratio was calculated of the P2R gene of interest (either $P2X_{1\text{-}7}$ or $P2Y_{1,2,4 \text{ and } 6}$) to a constitutively expressed house-keeping gene (HPRT). We could not detect significant levels (i.e. >0.5 arbitary units; AU) of $P2X_{2,3,5,7}$ and $P2Y_1$ mRNA under any experimental condition (n = 6). In contrast, significant amounts of mRNA (1-2 AU) were detected for $P2X_4$ and $P2Y_{2 \text{ and } 6}$ in CDs from rats on a 'normal' Na^+ intake. CDs from rats on a 'low' Na^+ diet showed a significant increase in abundance of $P2X_4$ and $P2Y_6$ mRNA (by 2-fold; n = 6, $P < 0.01$); CDs from rats maintained on a 'high' Na^+ diet showed a significant decrease in abundance of $P2Y_2$ mRNA (to less than 0.5 AU; n = 6); CD $P2X_{1 \text{ and } 6}$ and $P2Y_4$ mRNA levels were not significant on a 'normal' Na^+ diet, but were increased on a 'low' Na^+ diet (n = 6). However, there were no differences in mRNA expression between 'normal' Na^+ diet and hypertensive rats (n = 6). Thus, P2R mRNA expression levels change in the rat CD in response to changes in dietary Na^+, but not in DOCA-salt hypertensive rats. From these data it is unlikely that altered CD P2R function plays a role in this model of hypertension.

Wildman SS et al. (2005). J Am Soc Nephrol 16, 2586-2597.

Wildman SS et al. (2007). FASEB 21(6), A1328.

Supported by Wellcome Trust, British Heart Foundation and St Peter's Trust.

Where applicable, the authors confirm that the experiments described here conform with The Physiological Society ethical requirements.

PC9

Rhesus associated glycoproteins, RhBG and RhCG; investigating localisation and interactions in the kidney

A.C. Brown, S. Ashman and A.M. Toye

Biochemistry, University of Bristol, Bristol, UK

In healthy individuals excess acid generated from metabolism is excreted into the urine by specialised alpha-Intercalated cells (α-IC) of the distal tubule. These cells require the co-ordinated action of several proteins to adequately acidify the urine. One such protein, located at the blood-facing surface (the basolateral membrane) of the α-IC, is kidney anion exchanger 1 (kAE1), a truncated isoform of the red blood cell anion exchanger 1 (eAE1, Band 3). Specific mutations of the AE1 gene cause distal renal tubular acidosis (dRTA) demonstrating its essential role in urine acidification. We are interested in characterising interactions between kAE1 and other proteins that may play a role in regulating kAE1 trafficking or stabilise it at its basolateral membrane location. In the erythrocyte AE1 is known to be a fundamental component of an AE1-Rh membrane protein macrocomplex, which includes the Rhesus associated protein, RhAG. Importantly, the α-IC contains two RhAG homologues, RhBG and RhCG, that are thought to be implicated in acid secretion via ammonia transport. We have created novel RhBG and RhCG cell lines and antibodies to test our hypothesis that a similar RhBG or RhCG:kAE1 complex may exist in the kidney.

To independently confirm the location of RhBG and RhCG in the kidney we have created and polarised MDCKI cell lines stably expressing either human RhBG or RhCG tagged with C- or N-terminal GFP in the presence and absence of kAE1. We have shown that choice of location of the GFP tag on RhBG or RhCG can influence the polarised localisation of the proteins. The cell lines, and human kidney tissue, have been used to characterise

novel antibodies to RhCG that are now being used to investigate RhCG distribution and putative in vivo kAE1 co-localisation in human and mouse kidney. We are now utilising these novel cell lines to investigate the existence of a putative RhBG or RhCG:kAE1 interaction in the basolateral membrane. This cell model system will also allow for future investigation to define the physiological function of these transporters.

This work is funded by a Kidney Research UK and GlaxoSmithKline PhD studentship and a NHS Blood and Transplant Wellcome Trust Fellowship.

Where applicable, the authors confirm that the experiments described here conform with The Physiological Society ethical requirements.

PC10

High dietary sodium intake - an oxidative strress for the kidney?

E.J. Johns, B. O'Shaugnessy, S. O'Neill, B. Lane and V. Healy

Department of Physiology, University College Cork, Cork, Ireland

Mitochondrial respiration by the enzymes NAD(P)H, xanthine oxidase and others results in the production of reactive oxygen species (ROS) which comprise superoxide anions (O2-.), hydroxyl radicals (OH-) and hydrogen peroxide (H2O2). These species can damage other cellular proteins and degrade nitric oxide (NO) but their action is limited by the scavenging enzyme superoxide dismutase (SOD). In pathophysiological states, such as hypertension, heart failure, obesity and diabetes ROS production is increased reflecting a state of oxidative stress (Wilcox, 2002). What is less clear is how physiological challenges to cardiovascular and renal function may impact on ROS production. This was investigated by examining how the levels enzymes involved with ROS generation in the renal cortex and medulla responded to a period of elevated dietary sodium intake.

Male Wistar rats, 225-275g, were maintained on either a normal (0.3% Na) or a high salt diet (3% Na) for two weeks. Groups of 6-8 rats were placed in metabolic cages before and one and two weeks after dietary manipulation for 24h urine collections to allow estimation of fractional sodium and 8-isoprostane excretion. At the end of this period they were sacrificed, kidneys removed and separated into cortex and medulla/papilla, homogenized and proteins extracted. SOD and NAD(P)H expression and activity were measured. Data, means ±SEM, were analysed using Student's 't' test and significance taken at $P<0.05$.

After two weeks high sodium, fractional sodium excretion increased from 1.0±0.2 to 21±5 and 8-isoprostane excretion from 10±2 to 120±30 pg/kg/h (both $P<0.001$). NAD(P)H oxidase activity and protein expression increased some two-fold (both $P<0.05$) in the cortex, but not medulla in the rats subjected to the high salt diet. SOD activity was higher in the medulla than cortex in normal and high salt diet rats (both $P<0.05$). Protein expression of copper and zinc dependent SOD in cortex and medulla was similar in rats on both dietary regimes.

These findings show that a short period of elevated dietary sodium intake increases NAD(P)H activity and protein levels in the cortex and is associated with elevated 8-isoprostane excretion, consistent with a rise in ROS production. Importantly, the high salt intake did not change SOD activity and therefore scavenging potential. These observations support the view that this physiological challenge of high salt intake causes a modest oxidative stress.

Wilcox CS (2002). Hypertension Reports 4, 160-166

Where applicable, the authors confirm that the experiments described here conform with The Physiological Society ethical requirements.

PC11

High glucose affects structural and functional properties of human glomerular endothelial glycocalyx

A. Singh[1], V. Frieden[2], B. Haraldsson[2], P.W. Mathieson[1] and S.C. Satchell[1]

[1]Academic Renal Unit, University of Bristol, Bristol, UK and [2]Renal Unit, Sahlgrenska Academy,, Gothenburg University, Gothenburg, Sweden

Background:
The podocytes and the glomerular endothelial cells (GEnC) are the two cellular components of the glomerular filtration 'barrier'. We have recently shown that GEnC are covered by a thick layer of glycoproteins called glycocalyx which also acts a selective sieve to the passage of protein suggesting its contribution to the 'barrier' to protein *in vivo*. Diabetes, recognized by high glucose levels, is the commonest condition leading to dysfunction of this barrier leading to leakage of protein in the urine.
Aims:
To test the effects of high glucose on the structural components of GEnC glycocalyx and examine its functional relevance by analysing its barrier properties to the passage of water and albumin.
Methods:
We used conditionally immortalised human GEnC developed in our laboratory. For all experiments comparisons were made between cells cultured in control medium (with 5.5mM glucose and 20mM mannitol) and high glucose medium (25mM glucose). Expression of proteoglycan core proteins syndecan 1and 4, glypican-1, perlecan and versican was analysed by Western blotting. The expression of glycosaminoglycan chains was analysed by immunofluorescence and further quantified and characterized by radiolabelling studies (tritiated glucosamine and S^{35}). Barrier properties of GEnC monolayers were studied by real time trans-endothelial electrical resistance (TEER) and passage of labelled albumin.
Results:
High glucose reduced expression of total and sulphated glycosaminoglycan chains of glycocalyx by 55% and 62% respectively compared to controls ($n=4$, $p<0.0001$). Immunofluorescence further confirmed reduction in the heparan sulphate chains with preservation of endothelial junctions. There was however no significant change in the expression of proteoglycan core proteins. Functional studies showed no changes in passage of water and solutes after high glucose but a significant increase in the

Where applicable, the authors confirm that the experiments described here conform with The Physiological Society ethical requirements.

PC14

Inhibition of the CFTR Cl^- channel by loop diuretics

M. Ju, T.S. Scott-Ward, Z. Cai and D.N. Sheppard

Department of Physiology and Pharmacology, University of Bristol, Bristol, UK

Loop diuretics are widely used to inhibit the Na^+-K^+-2Cl^- cotransporter (Haas & Forbush, 2000). However, Venglarik (1997) demonstrated that loop-diuretics inhibit the cystic fibrosis transmembrane conductance regulator (CFTR) Cl^- channel. To understand better how loop diuretics inhibit CFTR, we studied furosemide, bumetanide, and two other agents xipamide and piretanide, which are structurally related to furosemide and bumetanide, respectively. We recorded CFTR Cl^- currents in inside-out membrane patches excised from C127 cells expressing wild-type human CFTR. The pipette (external) solution contained 10 mM Cl^- and the bath (internal) solution contained 147 mM Cl^-, 0.3 mM ATP and 75 nM PKA at 37°C; voltage was –50 mV. Data are means ± SEM of n observations and statistical analyses were performed using Student's paired t test.

When added to the internal solution, loop diuretics caused a reversible, concentration-dependent decrease in CFTR Cl^- current. For all agents tested, the concentration-response relationship was well fitted by the Hill equation with Hill coefficients of ~1. The rank order of potency for CFTR inhibition was xipamide (K_i = 45 ± 4 μM) ≥ bumetanide (K_i = 56 ± 11 μM) = piretanide (K_i = 58 ± 18 μM) ≥ furosemide (K_i = 71 ± 15 μM) (n = 5 for all agents).

To investigate further channel block, we used noise analysis. In the absence of furosemide, power density spectra of CFTR Cl^- currents were best fitted with two Lorentzian components with corner frequencies f_{c1} and f_{c2} of 1.17 ± 0.6 and 81 ± 10 Hz (n = 4), whereas in the presence of furosemide (100 μM), power density spectra were best fitted with three Lorentzian components with f_{c1}, f_{c2} and f_{c3} of 2.64 ± 1.38, 63 ± 25 and 312 ± 107 Hz (n = 4), respectively, suggesting that f_{c3} corresponds to the rapid binding and dissociation of furosemide to and from individual CFTR Cl^- channels. Consistent with this idea, furosemide (100 μM) caused a flickery block of CFTR decreasing both open probability (P_o: control, 0.41 ± 0.03; furosemide (100 μM), 0.17 ± 0.02; n = 6; $p < 0.01$) and single-channel current amplitude (i: control, –0.76 ± 0.01 pA; furosemide (100 μM), –0.63 ± 0.03 pA; n = 6; $p < 0.01$). Thus, our data demonstrate that loop diuretics inhibit CFTR, their potency approaches that of the widely used CFTR blocker glibenclamide and that furosemide acts an open channel blocker of CFTR.

Haas M & Forbush III B (2000). *Ann Rev Physiol* **62**, 515-534.

Venglarik CJ (1997). *Pediatr Pulmonol Suppl* **14**, 230.

We thank Dishman Pharmaceuticals & Chemicals Ltd and Sanofi-Aventis for generous gifts of xipamide and piretanide, respectively. This work was supported by the CF Trust.

Where applicable, the authors confirm that the experiments described here conform with The Physiological Society ethical requirements.

PC15

Anion transport across planar lipid membranes by an artificial anionophore

G. Magro[1,2], L.W. Judd[2], D.N. Sheppard[1] and A.P. Davis[2]

[1]Physiology, University of Bristol, Bristol, UK and [2]Chemistry, University of Bristol, Bristol, UK

Natural and artificial ion transporters consisting of transmembrane channels or carriers are well known. Most of the synthetic transporters concern cation transport, whereas less interest has been shown in anion transport so far. In previous work (Koulov et al. 2003), we demonstrated that a family of small molecules derived from cholic acid termed 'cholapods' bind anions with high-affinity, promote Cl- efflux from liposomes and ion transport across polarised MDCK epithelia (Koulov et al. 2003). Using excised inside-out membrane patches from giant liposomes, we compared the activity of cholapods with that of the cystic fibrosis transmembrane conductance regulator (CFTR) Cl- channel under the same conditions. Addition of cholapods caused a concentration-dependent increase in Cl- current, but no unitary events were observed.

We present here results obtained with a series of cholapods studied in planar lipid membranes (PLM). Membranes were formed by painting a mixture of POPE/Cholesterol (7/3) plus a known amount of cholapod. Using PLM, we have access to both sides of the membrane and thus to modify its environment. Thus, it has been possible to measure cholapod-mediated current under a series of conditions. Addition of cholapods in DMSO to the cis side of the membrane increased the observed current at an applied voltage (e.g. -100 mV). As the ion concentration was elevated the magnitude of cholapod-induced current saturated. Permeability experiments have been carried out and the transporters show good anion vs. cation selectivity, and also selectivity between anions. We interpret these data to suggest that cholapods can mediate anion transport across artificial lipid membranes by a carrier mechanism. Access to both sides of the membrane makes the PLM a potent technique to analyse the mechanism of action of synthetic anion transporters.

Koulov AV et al. (2003). Angew Chem Int Ed Engl 42, 4931-4933.

Supported by the BBSRC, EU, CF Trust.

Where applicable, the authors confirm that the experiments described here conform with The Physiological Society ethical requirements.

PC18

RT-PCR analysis of the expression of Cl^- channels in MDCK cells

X. Chen, H. Li, B. Liu, M. Ju and D.N. Sheppard

Dept. of Physiology & Pharmacology, The University of Bristol, Bristol, UK

Mardin Darby canine kidney (MDCK) cells are widely used as a model of renal epithelial ion transport. In previous work, we found that iodide efflux by type I MDCK cells was activated by cAMP and Ca^{2+} agonists and cell swelling, whereas that of type II MDCK cells was activated by cell swelling only (Li *et al* 2003). These data suggest that MDCK cells possess multiple different types of Cl^- channels. To test this hypothesis, in the present study, we used RT-PCR to explore the expression of Cl^- channels in MDCK cells. We investigated the expression of (i) CLCN2 and CLCN3, two members of the CLC family of Cl^- transporters, (ii) CFTR, the cAMP-stimulated Cl^- channel, (iii) bestrophin, the Ca^{2+}-activated Cl^- channel and (iv) TTYH2 and TTYH3, putative Ca^{2+}- and cell swelling regulated Cl^- channels.

We extracted total RNA from MDCK cells using RNAqueous isolation kit (Ambion). With DNAse treated RNAs, we synthesized and amplified cDNAs using the One Step RT-PCR kit (Qiagen). We designed primers for RT-PCR using Primer 3 software based on consensus sequences across species. We visualised DNA fragments after agarose gel electrophoresis by staining with ethidium bromide. Then, we purified RT-PCR products with the QIAquick PCR purification kit before sequencing the DNA fragments using the MWG nucleotide sequencing service. As controls, we examined the expression of β actin and performed reactions without a reverse transcription step to monitor contamination of samples by genomic DNA. Expression of each gene was examined in multiple samples from both cell types.

Both type I and type II MDCK cells expressed each of the different genes investigated. However, in the case of bestrophin, although DNA fragments of the expected size were obtained, the sequence of these fragments was not verified by nucleotide sequencing. With the exception of TTYH2, which was more abundant in type II MDCK cells, visual inspection of agarose gels suggested that each of the different genes examined were equally expressed in type I and type II MDCK cells. These data contrast strikingly with our functional data, which suggest that type I, but not type II, MDCK cells express Cl^- channels regulated by cAMP-dependent phosphorylation and the intracellular Ca^{2+} concentration. Future studies should explore the reason for the dichotomy between the molecular and functional expression of Cl^- channels in MDCK cells.

Li H and Sheppard DN (2003). *J Physiol.* **549**.P, 16P

X Chen was the recipient of a BBSRC Vacation Studentship. Supported by the CF Trust.

Where applicable, the authors confirm that the experiments described here conform with The Physiological Society ethical requirements.

PC19

The F508del mutation attenuates cyst formation by MDCK cells expressing wild-type human CFTR

H. Li[1], W. Yang[1], F. Mendes[2,3], M.D. Amaral[2,3] and D.N. Sheppard[1]

[1]Dept. of Physiology & Pharmacology, The University of Bristol, Bristol, UK, [2]Dept. of Chemistry & Biochemistry, University of Lisboa, Lisboa, Portugal and [3]National Institute of Health, Lisboa, Portugal

In previous work we demonstrated that inhibition of the cystic fibrosis transmembrane conductance regulator Cl^- channel (CFTR) retarded renal cyst growth (Li *et al.* 2004). To investigate the role of CFTR in cyst formation, we studied cyst formation by MDCK cells stably expressing wild-type human CFTR (WT-CFTR-MDCK) or loss-function mutation F508del (F508del-CFTR-MDCK) (Mendes *et al.* 2005). We also tested the effects of a specific CFTR blocker $CFTR_{inh}$-172 (Ma *et al.* 2002) on WT-CFTR-MDCK cyst formation.

For cyst formation assays, we seeded MDCK cells in 24-well plates containing collagen gel and cultured them with media containing 10% FBS and forskolin (10 μM) for 6 days. To study the effects of $CFTR_{inh}$-172 on cyst formation, we treated WT-CFTR-MDCK cells from day 0 with the drug at 10 μM (Ma *et al.* 2002). On day 6, we counted all cysts with a diameter > 50 μm in each well. Using digital images, we measured area of individual cyst with ImageJ software. Assuming that cysts are spherical in shape, we calculated cyst volume ($4/3 \times \pi \times r^3$). For cell proliferation assays, MDCK cells were seeded in 12-well plates containing MDCK media with 10% FBS and 10 μM forskolin in the absence or presence of $CFTR_{inh}$-172 (10 μM).

In the presence of forskolin, WT-CFTR-MDCK cells formed more cysts (9.2 ± 0.8, n = 37 wells) with larger volume (0.23 ± 0.02 mm^3, n = 265 cysts) compared to parental MDCK cells (2.0 ± 0.3, n = 24 and 0.10 ± 0.01 mm^3, n = 48, $P < 0.01$, Student's unpaired t-test). In contrast, F508del-CFTR-MDCK cells formed fewer cysts (0.4 ± 0.1, n = 27, $P < 0.01$ vs. parental MDCK cells) with smaller volume (0.02 ± 0.01 mm^3, n = 11, $P < 0.05$ vs. parental MDCK cells). $CFTR_{inh}$-172 (10 μM) reduced significantly both the number and volume of cysts formed by WT-CFTR-MDCK cells (3.7 ± 0.8, n = 15 and 0.08 ± 0.01 mm^3, n = 44, $P < 0.01$ vs. untreated WT-CFTR-MDCK).

Cell proliferation and fluid secretion are important factors affecting renal cyst formation (Sullivan *et al.* 1998). To exclude the possibility that differences in cyst formation were caused by variation in the rate of cell growth, we studied the proliferation of the three MDCK cell lines with the same conditions used for cyst formation assays. At day 6, there was no significant difference in cell numbers among all the experimental groups ($P > 0.05$). We interpret our data to suggest that wild-type human CFTR promotes renal cyst formation mainly through its role of mediating Cl^- secretion and hence, water transport into the cyst lumen. Either a loss-function mutation or a CFTR inhibitor attenuates greatly renal cyst formation.

Li H *et al.* (2004). *Kidney Int* **66**, 1926-1938.

Mendes F *et al.* (2005). *Cell Physiol Biochem* **16**, 281-290.

Ma T *et al.* (2002). *J Clin Invest* **110**, 1651-1658.

Sullivan LP *et al.* (1998). *J Am Soc Nephrol* **9**, 903-916.

Supported by the NKRF and CF Trust.

Where applicable, the authors confirm that the experiments described here conform with The Physiological Society ethical requirements.

PC20

Evidence for a role for ERK5 in EGF-induced renal epithelial cell survival - a possible role for MEF2C?

J.A. Browne[1], K. Paramasivam[1], D. Baines[2], M.E. C.Dockrell[1] and P. Colville-Nash[1]

[1]South West Thames Institute for Renal Research, St Helier Hospital, Carshalton, UK and [2]Department of Basic Medical Science, St George's Hospital Medical School, London, UK

Extracellular signal-regulated kinase-5 (ERK5) (previously known as BMK1) is an atypical MAP kinase. The exact role of ERK5 remains unknown however it is critically important in cell survival and differentiation as highlighted by the embryonic lethality of the ERK5 knock-out (Yan et al., 2003). ERK5 possess a transactivation domain and may act as a transcriptional coactivator by recruiting basal transcriptional machinery. ERK5 has been shown to induce its translocation to the nucleus, where it can activate the transcription factor, Myocyte enhancing factor-2C (MEF2C), inducing c-Jun expression (Kato et al. 1997). Hence the functions of MEF2 could be regulated through ERK5. ERK5 has been shown to be anti-apoptotic in endothelial cells (Pi et al. 2004) and to mediate the survival of neurones in the CNS via the activation of MEF2 (Liu et al., 2003; Shalizi et al. 2003). Inhibitors of the ERK1/2 pathway (PD 98059 or UO126) have been reported to inhibit ERK5. However previously we have shown that neither inhibitor reduce EGF-induced ERK5 in proximal tubule epithelial cells (PTECs). We therefore used siRNA to selectively knock down ERK5 and investigate the role of ERK5 in PTEC apoptosis.

Lysates of HKC-8 cells treated for 5 min with either EGF (10ng/ml) or vehicle (0.1% BSA) were used for Western blotting or subjected to Immunoprecipitation (for MEK5 and ERK5) prior blotting using antibodies targeting proteins of interest. ERK5 siRNA was optimised and a consistent knock-down of 60% was achieved. ERK5 siRNA (100nM) transfected cells were similarly treated but for 24h and caspase-3/7 activity measured as a measure of apoptosis.

Here we show that EGF-induced activation of ERK5 in PTEC is associated with increased association of MEK5 with not only ERK5 but also MEF2C. In addition, EGF inhibited staurosporine-induced apoptosis. siRNA knockdown of ERK5 significantly ($P<0.001$) increased apoptosis and EGF did not alter apoptosis in the presence of ERK5 siRNA.

Our work provides evidence that ERK5 may mediate EGF-induced cell survival in human PTEC. We present the first demonstration of MEF2C expression in PTEC and propose that it has a role in EGF-ERK5 cell survival.

Lijun Yan, Julia Carr, Peter R Ashby, Victoria Murry-Tait, Calum Thompson, and J Simon C Arthur (2003). BMC Dev Biol 3, 11.

Y Kato, V V Kravchenko, R I Tapping, J Han, R J Ulevitch, and J D Lee (1997). EMBO J 16(23), 7054–7066.

Pi X, Yan C, and Berk BC (2004). Circulation Research 94, 362-9.

Lidong Liu, Jane E. Cavanaugh, Yupeng Wang, Hiroyuki Sakagami, Zixu Mao and Zhengui Xia (2003). Proc Natl Acad Sci U S A 100(14), 8532–8537.

A. Shalizi, M. Lehtinen, B. Gaudilliere, N. Donovan, J. Han, Y. Konishi, and A. Bonni (2003). J Neurosci 23, 7326-7336.

Where applicable, the authors confirm that the experiments described here conform with The Physiological Society ethical requirements.

PC21

Differential dose-dependent BMP-7 signalling in PTECs and implication in fibrosis

R. Motazed, P. Colville-Nash, J.T. C Kwan and M.E. C Dockrell

Renal, South West Thames Institute For Renal Research, London, UK

Bone Morphogenic protein-7 (BMP-7) appears to maintain proximal tubule epithelial cells (PTECs) morphology in human adult kidney at levels which activates Smad 1. Reduced levels of BMP-7 exist in diabetic animal model of fibrosis and the effects of low dose BMP-7 which does not activate Smad 1 may correlate with the progression of this and other fibrotic diseases. Hence high dose BMP-7 which activates Smad 1 may reverse TGF-β induced fibrotic outcomes. We have previously described novel BMP-7-induced signalling in PTECs, at concentrations below those known to activate the Smad pathway. We have also investigated upstream, downstream signalling and cell survival and proliferation in response to low dose BMP-7. In addition this work investigates BMP-7 regulation of Smads and p38-MAP kinase signalling and modulation of TGF-β-induced fibrotic outcomes in adult human PTECs. We hypothesized that activation of Smad and p38 may be mutually exclusive.

Human Kidney Clone-8 (HKC-8) cells were treated with BMP-7 (2.5 and 200 ng/ml) at 5, 15 and 60 mins. Activation of p38, MKK3/6, MAPKAPK-2 and Smad signalling was studied by Western blot. Immunocytochemistry was used to look at the intracellular localisation of phoshpo-p38, MAPKAPK-2 and Smad 1 after treatment with 2.5 and 200 ng/ml of BMP-7. The effect of BMP-7 and p38 on cell apoptosis and proliferation of PTECs was measured with Caspase-Glo 3/7 and BrdU assay respectively. The effect of BMP-7 on TGF-β induced signalling and fibronectin (Fn) production was measured by ELISA.

BMP-7 activated Smad 1 at high concentration (200 ng/ml), but activated p38 at lower concentration (2.5 ng/ml). Nuclear localization of both Smad 1 and phospho-p38 is dependent on the concentration of BMP-7, 2.5 ng/ml resulting in nuclear phospho-p38 and 200ng/ml in nuclear Smad 1. We have also shown MKK3/6 to be the upstream of p38 and MAPKAPK-2 to be downstream following treatment with low dose BMP-7. BMP-7 (2.5ng/ml) did not significantly affect cell proliferation nor did it induce or modify staurosporin-induced apoptosis. High dose BMP-7 reduced TGF-β induced p38 production and significantly reduced TGF-β induced Fn secretion at 48 hours.